An automated procedure for estimating the leaf area index (LAI) of woodland ecosystems using digital imagery, MATLAB® programming and its application to an examination of the relationship between remotely sensed and field measurements of LAI

SIGFREDO FUENTES[AB*], ANTHONY R. PALMER[B], DANIEL TAYLOR[B], MALENIE ZEPPEL[B], RHYS WHITLEY[B], DEREK EAMUS[B]

[A]Plant Research Centre. University of Adelaide, Waite Campus, PMB 1 Glen Osmond, 5064, SA

[B]Institute for Water and Environmental Resource Management (IWERM), University of Technology, Sydney, NSW 2007. Australia.

*Corresponding author: sigfredo.fuentes@adelaide.edu.au.

ABSTRACT

Leaf area index (LAI) is one of the most important variables required for modelling growth and water use of forests. Functional structural plant models use these models to represent physiological processes in 3D tree representations. Accuracy of these models depends on accurate estimation of LAI at tree and stand scales for validation purposes. A recent method to estimate LAI from digital images (LAI_D) uses digital image capture and gap fraction analysis (Macfarlane *et al.* 2007b) of upward-looking digital photographs to capture canopy LAI_D (cover photography). After implementing this technique in Australian evergreen *Eucalyptus* woodland, we have improved the method of image analysis and replaced the time consuming manual technique with an automated procedure using a script written in MATLAB® 7.4 (LAI_M). Furthermore, We used this method to compare MODIS LAI values with LAI_D values for a range of woodlands in Australia to obtain LAI at the forest scale. Results showed that the MATLAB® script developed was able to successfully automate gap analysis to obtain

LAI_M. Good relationships were achieved when comparing averaged LAI_D and LAI_M (LAI_M = 1.009 – 0.0066 LAI_D; R^2 = 0.90) and at the forest scale, MODIS LAI compared well with LAI_D (MODIS LAI = 0.9591 LAI_D – 0.2371; R^2 = 0.89). This comparison improved when correcting LAI_D with the clumping index to obtain effective LAI (MODIS LAI = 1.0296 LAI_e + 0.3468; R^2 = 0.91). Furthermore, the script developed incorporates a function to connect directly a digital camera, or high resolution webcam, from a laptop to obtain cover photographs and LAI analysis in real time. The later is a novel feature which is not available on commercial LAI analysis softwares for cover photography. This script is available for interested researchers.

Key words: Leaf area index, *Eucalyptus*, digital imagery, MODIS LAI, MATLAB, remote sensing.

INTRODUCTION

Leaf area index (LAI) can be defined as the total one-sided area of leaf tissue per unit ground surface area (Watson 1947). LAI is an important parameter used to validate plant architectural models (De Reffye *et al.* 1995). Accurate estimates of LAI are also important for functional structural plant models, whilst leaf area strongly influences rates of evapotranspiration and photosynthesis of trees (Nemani et al. 1993; Villalobos et al. 1995). Consequently, estimation of this parameter is also important for modelling forest growth and water use (Macfarlane *et al.* 2007b), since it determines the productivity and physical and biophysical interactions between land surfaces and the atmosphere (Chen and Cihlar 1995). Finally, accurate estimations of LAI are critical to scale-up leaf-based physiological measurements to the whole tree (Ewert 2004), tree-based measurements (e.g. sap flow) to the stand scale (Whitley *et al.* 2007; Zeppel *et al.* 2007; Zeppel *et al.* 2004) and to scale from regional to continental processes of land surface-atmosphere exchange (Lu and Shuttleworth 2002; Ewert 2004).

Direct versus indirect LAI measurement

Direct measurements of LAI (allometry or litterfall) are difficult and time consuming to perform on trees (Cutini *et al.* 1998). Furthermore, these methods do not easily allow a representative spatial and temporal resolution of LAI at the forest stand scale (Chason *et al.* 1991). Consequently, ground-based indirect methods have been developed and are more commonly used to estimate LAI. Typically these are based on measurements of radiation transmission through the canopy (Bréda 2003), for example the Licor-2000 (Plant canopy analyser; Li-COR, Lincoln, NE) (Arias *et al.* 2007; Bréda 2003; Cutini *et al.* 1998; Villalobos *et al.* 1995). However, the cost of the

Licor-2000 can be prohibitive (Macfarlane *et al.* 2007b) and can underestimate LAI between 10-40% (Macfarlane *et al.* 2000) in forests.

Fisheye versus cover digital photography

Fisheye photography or hemispherical methods have been proposed as a less costly alternative to direct measurements. These techniques measure the gap fraction at more than one zenith angle. However, the downside of these techniques is that in reality, estimates of the light extinction coefficient (k) are usually flawed owing to foliage clumping, inaccurate gap fraction retrieval and the inclusion of woody structures in the estimation of leaf area. An improved fisheye technique can be achieved using "fullframe fisheye photography", which increases the resolution and accuracy of gap fraction retrieval (Macfarlane *et al.* 2007a). Most recently, estimation of LAI indirectly using digital or cover photography and gap fraction analysis have been developed and this provides an accurate and rapid estimation of LAI (Macfarlane *et al.* 2007b). Furthermore, studies comparing hemispherical, fullframe fisheye and cover photography (digital) have concluded that the later is the best option for routine, indirect measurements and monitoring of LAI in broadleaf forests (Macfarlane *et al.* 2007b). Furthermore, the cover photography method outperforms fisheye photography, since the former can be applied during daylight hours, are of much higher resolution (less sensitive to photographic exposure), sky luminance is more even and the narrow viewing angle is better suited to small rectangular plots. However, the cover photography method could not be automated using commercially available analysis software (Macfarlane *et al.* 2007a; Macfarlane *et al.* 2007b; Macfarlane *et al.* 2007c)

Commercially available software for LAI analysis

The hemispherical or fullframe fisheye photography techniques require complicated analysis and specialised software (Bréda 2003; Frazer et al. 2001; Macfarlane et al. 2007a; Macfarlane et al. 2007b). The majority of this software is commercially available (some are freeware: *F*) to researchers, such as: Hemiview, Hemiphot, GLA, DHP-TRACWin, CANEYE (*F*) and WinSCANOPY (Regent Instruments, Ste-Foy, Quebec). This software was mainly developed to analyse hemispherical photography and fullframe fish eye photography (Macfarlane *et al.* 2007b). In contrast, the cover photography method uses normal digital cameras and upward-looking digital photographs to capture canopy LAI (LAI_D) and analyses these images at a single zenith angle (0^o – 15^o), using commercial image processing software (Photoshop 7.0 ®). This process is time consuming (5 min per image) and hence costly when analysing 50 or more images for a single site. This technique also introduces user subjectivity when selecting adequate large gap fractions and blue light thresholds between canopy and sky for each image. With the improved availability of cost effective high resolution digital cameras there is an incentive to further automate this technique. Recently, WinSCANOPY have incorporated analysis of cover photography, which is not fully automated. A comparison between WinSCANOPY and the method using Adobe Photoshop 7.0 (LAI_D, which is used as a baseline in this study) was tested by Macfarlane *et al.* (2007c). This study found that results between WinSCANOPY and Photoshop have little difference in LAI estimation; however, they varied from individual images, as evidenced by the small correlation coefficients between the two methods for crown porosity and the clumping index (Macfarlane *et al.* 2007b).

MODIS-LAI estimates

At the forest and catchment scale, LAI estimates can be derived from satellite spectral reflectance measurements (Nemani *et al.* 1993, Palmer et al. 2008). This method is based on either the strong relationship between LAI and NIR/RED ratio (Carlson and Ripley 1997; Peterson *et al.* 1987) or the normalised difference vegetation index (NDVI). High correlations between NDVI and LAI have been found for non-continuous herbaceous crops, such as grapevines (Johnson 2003) and forests (Lu and Shuttleworth 2002; Peterson *et al.* 1987). An alternative is to implement radiative transfer (RT) simulations, which simulates average (average what??) over satellite pixel RT field, such as the Moderate resolution Imaging Spectroradiometer (MODIS) LAI algorithm (Huang *et al.* 2008). The MODIS 8-day 1 km LAI/FPAR product (MOD15A2 Collection 4) (Knyazikhin *et al.* 1998) is an improvement on the simple band ratio products and was available for the present study period from NASA's Distributed Active Archive Centre. Very recently collection 5 has been released and this increases the amount of high quality retrievals over broadleaf forests A suitable ground based LAI measurement is necessary to validate and assess uncertainties associated with satellite-derived products such as MODIS LAI (Tian *et al.* 2002).

In this paper we describe an image analysis tool written in MATLAB® 7.4 and compare results using this tool (LAI_M) with LAI_D. The tool developed is able to batch-process digital images using gap fraction analysis, making the procedure automatic (on clear or fully overcast day images) or semi-automatic (on patchy cloudy day images). We also compared LAI_D with MODIS LAI values for a range of woodlands in New South Wales (NSW) and Western Australia (WA) to validate

MODIS LAI data at the forest scale. Since digital images and analysis includes trunks and brunches, it is argued that estimates correspond to Plant Area Indices (PAI) rather than LAI (Bréda 2003). However, to maintain a consistent nomenclature we will use LAI for LAI_D, LAI_M and MODIS LAI in results.

MATERIALS AND METHODS

2.1. Site locations

Data included in this study were obtained from sites described in Table 1.

Table 1: Sites of 1 ha approximately in NSW and WA were used to validate the script developed (marked with *) and MODIS LAI results (marked with * and **).

Site Name	Location	State
Castlereagh*	33°39'41.54"S; 150°46'58.27"E	NSW
Bago*	35°39'20.6"S; 148°09'07.5"E	NSW
Paringa*	31°25'16.7”S; 150°36'28”E	NSW
Sunnycorner*	33°23'36.63"S; 149°52'44.47"E	NSW
Hornsby*	33°40'3"S; 151°10'32"E	NSW
Condobolin**	33° 3'12.40"S; 146° 6'53.79"E	NSW
Quairadin**	32°46'18.82"S; 117° 6'26.48"E	WA
Wandoo NP**	32°45'0.02"S; 116°55'42.00"E	WA

2.2. Digital image acquisition

A Nikon® Coolpix 995 (3,145,728 pixels in total) mounted on a tripod with a bubble level to obtain images at the zenith angle was used to aquire digital images from all sites. Images were collected at 1.5 m from the ground as FINE JPEG. The camera was

set to automatic exposure using a F2 lens, which gives a zoom angle of approximately 35^{o} across the diagonal, or about $0\text{-}15^{o}$ zenith angle range. In all sites, five images every 10 m were taken over five linear transect located 10 m apart. This procedure was repeated twice per site, giving a total of 50 images per site. Images were collected in August 2006 at all sites.

2.3. MATLAB® script development

We used MATLAB® 7.4 (The Mathworks, Inc) and the Image Processing Toolbox ™ to generate a script to batch process numerous upward-looking digital images (at least 50 per site). The objective was to automate the estimation of LAI from five different woodland sites within NSW (Table 1) and to compare results of LAI_M with LAI_D and MODIS LAI. The user inputs answers to seven questions (Table 2) made by the script at the start of each batch process.

Table 2: Questions from the script developed to be answered by the user at the beginning of the analysis.

Question	Script outputs	User input
a	Name of files	Alphanumeric
b	Initial image	Numeric (1 – n)
c	Last image	Numeric (1 – n)
d	Number of sub-divisions	Numeric (1 – n)
e	Gap fraction threshold	Numeric (0 – 1)
f	Light extinction coefficient	Numeric (0 – 1)
g	Number of approximations	Numeric (1 – n)

2.3.1. Filtering clouds from images

A binary (black and white) image was required to simplify gap fraction analysis. However, when trying to convert an RGB (red – green – blue) patchy cloud sky image (Fig. 1a) to a binary image (Fig. 1b) without filtering it tends to include clouds as leaf cover, leading to overestimations of LAI_M. To overcome this, the image colour and brightness components where analysed separately: Figures 2a (blue), 2b (green), 2c (red), 2d (hue), 2e (saturation) and 2f (intensity). The best cloud filters where the blue (Fig. 2a) and intensity (Fig. 2f) components, since they gave the best contrast between foliage cover and sky plus clouds.

2.3.2. Selecting luminance threshold

The blue band (450 – 495 nm) of each image was extracted as a histogram and explored to identify a suitable threshold between foliage and sky (Fig. 3). In this procedure, the selection of a suitable luminance value threshold (T) from the blue band histograms can be fully automated for numerous images (for clear or completely overcast days) or manually generated for each image (for patchy cloud days). After assigning a suitable T (cursor selection), the image is transformed into a binary image for gap analysis. In the program, there is an option (Question g) to give the user a number of attempts (1 – n) to select an accurate luminance threshold from the blue image component. This is done by viewing the original RGB image and the binary image side by side (Fig. 1) to see whether small gaps were missed or considered in filtered binary image. This feature, which helps to avoid over- or under-estimates of LAI_M, is not readily available in Photoshop® 7.0 or commercial softwares, such as WinSCANOPY.

2.3.3. Images gap analysis

The script developed performs gap analysis by automatically dividing each binary image into a number of sub-images defined by the user (Question d). From each sub-image, the program counts the total of pixels corresponding to sky (S) and leaves (L). A big gap is considered when the ratio S/L in each sub-image is larger that a user-specified value (Question e). When this occurs, the pixel count for S is added to the big gap count for that particular full image. If the ratio observed is smaller than the user-specified value for a specific sub-image, the pixel count contribution to the total big gap count of that particular image is equal to zero. A sensitivity test was performed using 10 random images per site and subdividing each image by 3x3 (n=9); 4x4 (n=16); 5x5 (n=25) and 6x6 (n=36). No significant differences were seen in the LAI_M obtained at different subdivisions (data not shown). Therefore, it was decided to divide all images at 3x3 (n=9) subdivisions to optimise data analysis time.

To analyse 50 images automatically, the script took approximately ten minutes using an Apple Macbook® Core Duo with 2.0 Gb. RAM at 2.3Ghz. Individual image analysis timing depended of the number of approximations selected by the user. Considering this number as three, it takes 1 minute approximately to analyse a single image. Also, a big gap threshold of 0.75 was the most appropriate for all images, since it gave the best comparison with LAI_D (LAI_D between 0.7 – 1.7).

The fractions of foliage projective cover **(f_f)**, crown cover **(f_c)** and crown porosity **(Φ)** are calculated from Mcfarlane *et al.* (2007b) as:

$$f_c(\%) = 100\frac{1-\mathrm{lg}}{\mathrm{tp}} \qquad \textbf{[1]}$$

$$f_f(\%) = 100\frac{1-\mathrm{tg}}{\mathrm{tg}} \qquad \textbf{[2]}$$

$$\Phi = \frac{f_f}{f_c} \quad \textbf{[3]}$$

Where lg = large gap pixels and tp = total gap pixels

LAI_M is calculated from Beer's Law, assuming an extinction co-efficient (k) of 0.5, which is suitable for eucalypt trees (Macfarlane *et al.* 2007b), (this value can be altered in the script Question f):

$$LAI_M = \frac{-f_c \ln \Phi}{k} \quad \textbf{[4]}$$

and the clumping index at the zenith, **Ω(0)**, was calculated as follows:

$$\Omega(0) = \frac{(1-\Phi)\ln(1-f_f)}{\ln(\Phi) f_f} \quad \textbf{[5]}$$

The clumping index is a correction factor to obtain effective LAI (LAI_e), which is the product of:

$$LAI_e = LAI_M \times \Omega(0) \quad \textbf{[6]}$$

Equation 5 describes the non-random distribution of canopy elements. If **Ω(0) = 1**, means that the canopy displays random dispersion; for **Ω(0) > or < 1**, the canopy is defined as clumped. LAI_e was not considered for the script development and results

presented in this paper; however it is available to be calculated in the last version of the program and was used to validate MODIS LAI data.

After image analysis, the script stores all the calculated parameters (LAI_M, f_f, f_c, Φ, $\Omega(0)$ and LAI_e) in a .txt file, which can be readily read by Excel®. The same equations [1 – 6] were used to calculate LAI_D using Adobe PhotoShop® 7.0 and the methodology described in Macfarlane *et al*. (2007b).

2.4. MODIS LAI analysis

Following the capture of digital images and determination of LAI_D for eight examples of *Eucalyptus* woodlands in NSW and WA (Table 1), we assessed the relationship between LAI_D and MODIS LAI products for each of the ground measurements. We extracted the 8-day 1 km MODIS LAI data for NSW and WA from the MODIS distributed archive and imported these into a GIS software package (IDRISI®; Clark Labs) (Figs. 6a and 6b). The ground sampling sites were established along a precipitation gradient (450 – 1400 mm) in NSW and WA. 8-day MODIS LAI values for ground sampling stations (of approximately 1 ha) were extracted using a data-drill. At each ground sampling station, LAI_D was calculated from at least 50 randomly collected images from the 1 ha stations within the 1 km MODIS pixel. Individual modelled MODIS LAI values for each sampling occasion were selected from the 8-day image closest to the date of the LAI_D sampling event. Although seasonal variations in MODIS LAI was apparent at each sampling site (i.e. range from LAI 1 to 4 in wet sites), the ground sampling events coincided with periods when MODIS LAI closely approximated LAI_D. The ground sampling excluded the contribution of understorey LAI, and was conducted during the dry season when the contribution of

the understorey would have been at its minimum.

2.5 Statistical analysis

To compare the performance of the script developed (LAI_M) and MODIS LAI with the baseline data (LAI_D), linear regression analyses among LAI_D, LAI_e and LAI_M; MODIS LAI were undertaken. A sensitivity analysis of LAI_M to T was conducted considering a variation of T of maximum $\delta T = +20$ and minimum $\delta T = -30$ (Fig. 7). Images taken on clear days conditions (n = 50) and on patchy cloudy day conditions (n = 30) were selected for the sensitivity analysis. Patchy cloudy days were avoided for data collection due to high variability in luminosity. Therefore, this explains the lower number of images on patchy cloudy days. The statistical analysis was done using MATLAB® 7.14 and the Curve Fitting Toolbox ™.

RESULTS AND DISCUSSION

LAI estimations using the script developed

The automated procedure to analyse digital images using the script resulted in a good averaged LAI_M compared to the averaged LAI_D for five sites (Figure 4, open circles) ($LAI_M = 1.009 – 0.0066\ LAI_D$; $R^2 = 0.90$). Standard errors were also similar between LAI_D and LAI_M. When patchy clouds were present in the images, the manually generated threshold was more appropriate to obtain accurate individual LAI_M from single images when compared to LAI_D (i.e. $LAI_M = 0.95\ LAI_D$; $R^2 = 0.95$, from 50 images; Hornsby site, data not shown). All sites showed mostly clumped canopies (at different levels) as can be seen in Fig. 5 ($\Omega(0) < 1$), with averaged minimum values of 0.6 for Castlereagh and maximum of 0.84 for Bago. The averaged $\Omega(0)$ considering

all sites was 0.78. This makes clear that corrections using the clumping index (using eq. 6) need to be introduced in the calculation of LAI_M and LAI_D to obtain LAI_e.

According to Bréda (2003), PAI rather than LAI terminology should be used for techniques using digital photography, since woody area (trunks and branches) is included in the analysis contributing to overestimations of LAI. However, the largest woody contributions in LAI_D (overestimations) are associated to images close to the main stem of tall trees. In contrast, using this technique in woodlands where species with lightly coloured trunks (e.g. Ghost gums (*Eucalyptus papuana*)) are mostly present, could contribute to under-estimations of LAI_D, since these stems can be mistaken for sky in the script filtering method if the fully automated routine proposed in this paper is used. Using the manual technique can remove this source of error. However, alternatively, images can be taken a couple of metres away from such stems to minimise woody inclusion and avoiding times of the day when trunks or branches receive direct sunlight. Finally, corrections for woody area are considered smaller for the digital image technique, than hemispherical photography (wide angle: $0 - 57^o$), since the narrow angle of digital images ($0\text{-}15^o$) reduces inclusion of stems and therefore their contribution to LAI_D (Kucharick et al. 1997).

The choice of a suitable T value, within the blue component of an image, is also critical to avoid over- or under-estimations of LAI_D (Macfarlane *et al*. 2007b). Therefore, the image comparison tool available within the script (Fig. 1a and 1b) is very useful to avoid errors in the LAI_D calculation. Suitable T values are very similar within images taken on clear or completely overcast days (Fig. 7a). An individual analysis of 2-5 images will be enough to obtain a common threshold for batch-analysis of images taken on these weather conditions. The other critical factors for

LAI_D calculations are crown cover (f_c) and porosity (Φ), which are highly dependant of the visual selection of large, between-crowns gaps. Using the script developed, operator subjectivity can be avoided when selecting large gaps through calibration of sub-image size and gap fraction ratio for different types of woodlands. This calibration is readily available for the script from other studies using digital photography compared to allometric measurements. Therefore, one of the most important advantages of the methodology described here is that images can be analysed using different gap and image analysis techniques. This is in contrast to most commercial ground based LAI analysers (such as Licor2000) which only provide the processed output and not the unprocessed data.

A useful feature of the script that was also developed was to acquire images using a high resolution web-cam attached to a laptop for in-field real-time digital image acquisition and application of the analysis as described in this paper. This feature is not available on commercial softwares to analyse cover photography (Adobe Photoshop 7.0 and WinSCANOPY). The script developed in this study is available to interested researchers with access to MATLAB©, the Image Analysis Toolbox® and Image Acquisition Toolbox®. An .exe version of the software will be available in the future as a Graphic User Interface (GUI) after compiling the script to run the program independently of MATLAB® in any personal computer.

LAI estimations using MODIS LAI

The regression MODIS LAI = 0.9591 LAI_D – 0.2371 (R^2 = 0.89) describes the relationship between LAI_D and MODIS LAI for the eight sites examined (Fig. 4, filled circles). For most of the sites, MODIS LAI tended to slightly overestimate LAI_M. We

attribute this result to the fact that MODIS LAI includes the LAI of the understorey whilst LAI_D does not. Although we used dry season MODIS LAI in the comparison, an averaged contribution of the order of 15% understorey to total site LAI for dry season images is to be expected (unpublished observations). When including the $\Omega(0)$ in the LAI_D calculation, the linear regression describing the LAI_e *versus* MODIS LAI relationship improved (MODIS LAI = 1.0296 LAI_e + 0.3468; R^2 = 0.91). Despite this, MODIS LAI was consistently larger than LAI_e (Fig. 4, open triangles). In this case, a total mean understorey contribution of 17% was observed, which did not significantly change from uncorrected LAI_D measurements. Another source of discrepancy between LAI_D and MODIS LAI is the accuracy of collection 4 used in this study. Collection 5 has been released recently, which can achieve better agreement of retrieved and measured ground LAI. Digital imagery analysis and availability of foliage clumping estimates can provide a useful LAI_D comparison with other methods, such as MODIS LAI (collection 5), to examine the understorey contribution to total forest LAI. Consequently, understorey LAI contribution can easily be incorporated in LAI_D measurements when capturing images at 30 cm from the ground rather than 1.5 m, or at both heights for comparative purposes. If the MODIS LAI product 5 is to become more universally applicable outside of evergreen woodland and forest, robust and efficient methods for estimating grass and understorey contribution need to be improved and automated. He *et al* (2007) report that two conventional LAI instruments (LAI 2000 Plant Canopy Analyser and AccupPAR Ceptometer) consistently underestimate grass LAI relative to destructive measurement.

Seasonal differences in LAI can be clearly seen using MODIS data and a GIS program (IDRISI®; Clark Labs.) for summer (Fig. 6a; 17th of January 2006) and spring (Fig. 6b; 30th of September 2006). A higher MODIS LAI is shown in January for woodland locations around NSW close to Sydney (MODIS LAI = up to 4.5) (Fig. 6a). A lower value for MODIS LAI (up to 2.5) was reached in spring for most of the woodland area seen in the figure (Fig. 6b).

Sensitivity analysis of LAI_M to T

A sensitivity analysis on LAI_M to T was performed to assess the error associated to mis-detection of a suitable T_{min} for global LAI_M analysis. Fig. 7 shows the blue layer histograms corresponding to 50 images obtained in clear day conditions (Fig. 7a) and 30 images in cloudy day conditions (Fig. 7b). Frequency distribution of the blue layer luminance was more uniform for clear days rather than cloudy days. Therefore, it is easier to select a suitable common T (Tmin = 130; Fig. 7a) for clear days for complete automation of image analysis using the script developed. On the contrary, selecting a common T for cloudy days could lead to an over or underestimation of LAI_M for individual images (Tmin = 100) and the selection is more difficult from the histogram showed in Fig. 7b. The semi-automatic method is recommended for images taken under patchy cloudy day conditions (see 2.3.1 and 2.3.2). Fig. 8 and Table 2 show the results of the sensitivity test for clear and patchy cloudy day conditions. The sensitivity of LAI_M to T increases with the magnitude of error of selection of T (δT) for both clear and patchy cloudy day images. Dispersion of data points is lower for clear days (Fig. 8a) compared to patchy cloudy days (Fig. 7b). In the later case the magnitude of error in selecting a suitable common T is considerable higher compared to clear days as can be seen by comparing the correlation coefficients (r^2), root mean

square error (RMSE) and the standard error of estimates (SEE) (Table 2). Average RMSE = 0.02; SEE = 0.018 and r^2 = 1.0 were found for clear days, and RMSE = 0.07; SEE = 0.21 and r^2 = 0.96 for cloudy days. There was no considerable change in the slopes (b) obtained in the sensitivity test for cloudy days compared to clear days, since b is more dependant of the levels of misdetection errors selected for the sensitivity analysis (δT), which were the same for both luminance conditions studied. A maximum error of 4% from T_{min} selected (δT = +10) (considering a maximum value of T = 250; Fig. 3) did not affect considerably LAI_M = 0.53 compared to LAI_D = 0.49, for clear days (Table 2). The Tmin selected for clear days resulted in LAI_M = 0.49 compared to LAI_D = 0.49. Therefore, it is easier to select a suitable T for these conditions. These results show that images including patchy clouds (Fig. 1) require the semi automated procedure for more accurate LAI_M estimations on individual images. On the contrary, for clear days or completely overcast days, a common selection of T from the blue layer histograms (Fig. 7a) may allow a maximum of 4% error in the selection of a suitable T value for fully automated analysis.

For patchy cloudy day conditions, a common T value and considering δT = 4% error, results between LAI_M and LAI_D where similar (LAI_M = 0.68; SD = 0.55 compared to LAI_D = 0.68; SD = 033). This means that a suitable T corresponded to T_{min} = 110 for these conditions. However, the correlation from individual pictures was lower (r^2 = 0.78; b = 0.84; RMSE = 0.34; SEE=0.37) than results using the semi automated method for individual images: LAI_M = 0.68; SD = 0.40; LAI_D = 0.68; SD = 0.33 (r^2 = 0.95; b = 0.91; RMSE = 0.12; SEE=0.62).

CONCLUSIONS

We conclude that digital image acquisition, coupled with MATLAB® image data analysis, provides a rapid, robust, cheap and simple method for determining the LAI of tree canopies. Furthermore, we conclude that for evergreen woodland, where seasonal understorey growth is limited due to seasonal or stochastic drought, the MODIS LAI product provides a useful surrogate for LAI_D. However, as the contribution of the understorey to total site LAI increases, this is increasingly untrue. Renewed efforts to improve estimates of understorey LAI, together with the results from the script developed, will improve the quality of input of LAI into functional structural plant models and validation for retrieved MODIS LAI (collection 5).

AKNOWLEDGMENTS

We thank Chris Hunt from Agresearch, Grasslands in New Zealand for his technical support.

REFERENCES

Arias D, Calvo-Alvarado J, Dohrenbusch A (2007) Calibration of LAI-2000 to estimate leaf area index (LAI) and assessment of its relationship with stand productivity in six native and introduced tree species in Costa Rica. *Forest Ecology and Management* **247**, 185-193.

Bréda NJJ (2003) Ground-based measurements of leaf area index: a review of methods, instruments and current controversies *Journal of Experimental Botany* **54**, 2403-2417.

Carlson TN, Ripley DA (1997) On the relation between NDVI, fractional vegetation cover, and leaf area index. *Remote Sensing of Environment* **62**, 241-252.

Chason JW, Baldocchi DD, Huston MA (1991) A comparison of direct and indirect methods for estimating forest canopy leaf area. *Agricultural and Forest Meteorology* **57**, 107-128.

Chen JM, Cihlar J (1995) Plant canopy gap-size analysis theory for improving optical measurements of leaf-area index. *Applied Optics* **34**, 6211-6222.

Cutini A, Matteucci G, Mugnozza GS (1998) Estimation of leaf area index with the Li-Cor LAI 2000 in deciduous forests. *Forest Ecology and Management* **105**, 55-65.

De Reffye P, Houllier F, Blaise F, Barthelemy D, Dauzat J, Auclair D (1995) A model simulating above- and below-ground tree architecture with agroforestry applications. *Agroforestry Systems* **30**, 175-197.

Ewert F (2004) Modelling Plant Responses to Elevated CO2: How Important is Leaf Area Index? *Annals of Botany* **93**, 619-627.

Frazer GW, Fournier RA, Trofymow JA, Hall RJ (2001) A comparison of digital and film fisheye photography for analysis of forest canopy structure and gap light transmission. *Agricultural and Forest Meteorology* **109**, 249-263.

He, Y. H., X. L. Guo, et al. (2007). Comparison of different methods for measuring leaf area index in a mixed grassland. *Canadian Journal of Plant Science* **87**, 803-813.

Huang D, Knyazikhin Y, Wang W, Deering DW, Stenberg P, Shabanov N, Tan B andMyneni RB (2008) Stochastic transport theory for investigating the three-dimensional canopy structure from space measurements. Remote Sensing of Environment 112, 35-50.

Johnson LF (2003) Temporal stability of an NDVI-LAI relationship in a Napa Valley vineyard. *Australian Journal of Grape and Wine Research* **9**, 96-101.

Knyazikhin, Y, Martonchik, JV, Myneni, RB, Diner, DJ, Running, SW. 1998 Synergistic algorithm for estimating vegetation canopy leaf area index and fraction of absorbed photosynthetically active radiation from MODIS and MISR data *Journal of Geophysical Research-Atmospheres* **103**: 32257-32275

Kucharik, C.J., Norman, J.M., Murdock, L.M., 1997. Characterising canopy nonrandomness with a multiband vegetation imager (MVI). *Journal of Geophysical Research* **102** (D24), 29, 455-29, 473.

Lu L, Shuttleworth WJ (2002) Incorporating NDVI-Derived LAI into the Climate Version of RAMS and Its Impact on Regional Climate. *Journal of Hydrometeorology* **3**, 347-362.

Macfarlane C, Arndt SK, Livesley SJ, Edgar AC, White DA, Adams MA, Eamus D (2007a) Estimation of leaf area index in eucalypt forest with vertical foliage, using cover and fullframe fisheye photography. *Forest Ecology and Management* **242**, 756-763.

Macfarlane C, Coote M, White DA, Adams MA (2000) Photographic exposure affects indirect estimation of leaf area in plantations of Eucalyptus globulus Labill. *Agricultural and Forest Meteorology* **100**, 155-168.

Macfarlane C, Hoffman M, Eamus D, Kerp N, Higginson S, McMurtrie R, Adams M (2007b) Estimation of leaf area index in eucalypt forest using digital photography. *Agricultural and Forest Meteorology* **143**, 176-188.

Macfarlane C, Grigg A, Evangelista C (2007c) Estimating forest leaf area using cover and fullframe fisheye photography: Thinking inside the circle. *Agricultural and Forest Meteorology* **146**, 1-12.

Nemani R, Pierce L, Running S, Band L (1993) Forest ecosystem processes at the watershed scale: sensitivity to remotely-sensed Leaf Area Index estimates. *International Journal of Remote Sensing* **14**, 2519 - 2534.

Peterson DL, Spanner MA, Running SW, Teuber KB (1987) Relationship of thematic mapper simulator data to leaf area index of temperate coniferous forests. *Remote Sensing of Environment* **22**, 323-341.

Tian Y, Woodcock CE, *et al.* (2002) Multiscale analysis and validation of the MODIS LAI product: II. Sampling strategy. *Remote Sensing of Environment* **83**, 431-441.

Villalobos FJ, Orgaz F, Mateos L (1995) Non-destructive measurement of leaf area in olive (Olea europaea L.) trees using a gap inversion method. *Agricultural and Forest Meteorology* **73**, 29-42.

Watson DJ (1947) Comparative Physiological Studies on the Growth of Field Crops: I. Variation in Net Assimilation Rate and Leaf Area between Species and Varieties, and within and between Years. *Annals of Botany* **11**, 41-76.

Whitley R, Zeppel M, Armstrong N, Macinnis-Ng C, Yunusa I, Eamus D (2007) A modified Jarvis-Stewart model for predicting stand-scale transpiration of an Australian native forest. *Plant and Soil*. DOI 10.1007/s11104-007-9399-x

Zeppel M, Macinnis-Ng C, Ford C, Eamus D (2007) The response of sap flow to pulses of rain in a temperate Australian woodland. *Plant and Soil*. DOI 10.1007/s11104-007-9349-7

Zeppel MJB, Murray BR, Barton C, Eamus D (2004) Seasonal responses of xylem sap velocity to VPD and solar radiation during drought in a stand of native trees in temperate Australia. *Functional Plant Biology* **31**, 461-470.

FIGURES

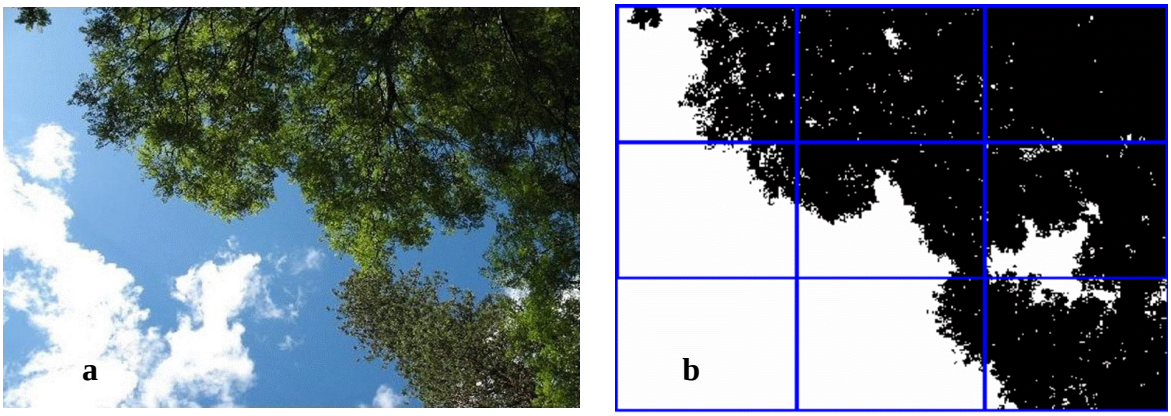

Figure 1. (a) Typical upward looking digital image in a patchy cloudy day. (b) Filtered binary image to avoid cloud inclusion in LAI_M analysis. Gap analysis considering nine image sub-divisions at question d = 3 (3 x 3 or n = 9).

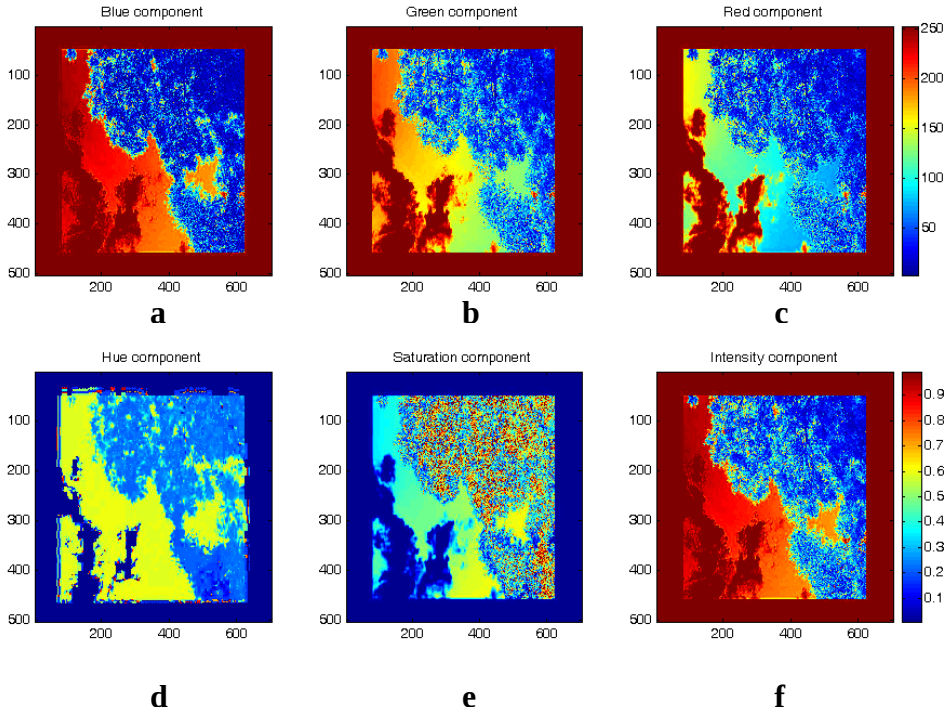

Figure 2. Image components separation using MATLAB® to obtain a cloud filtering rule for the script written in MATLAB®. (a) Blue and (f) intensity component were best suited for cloud filtering.

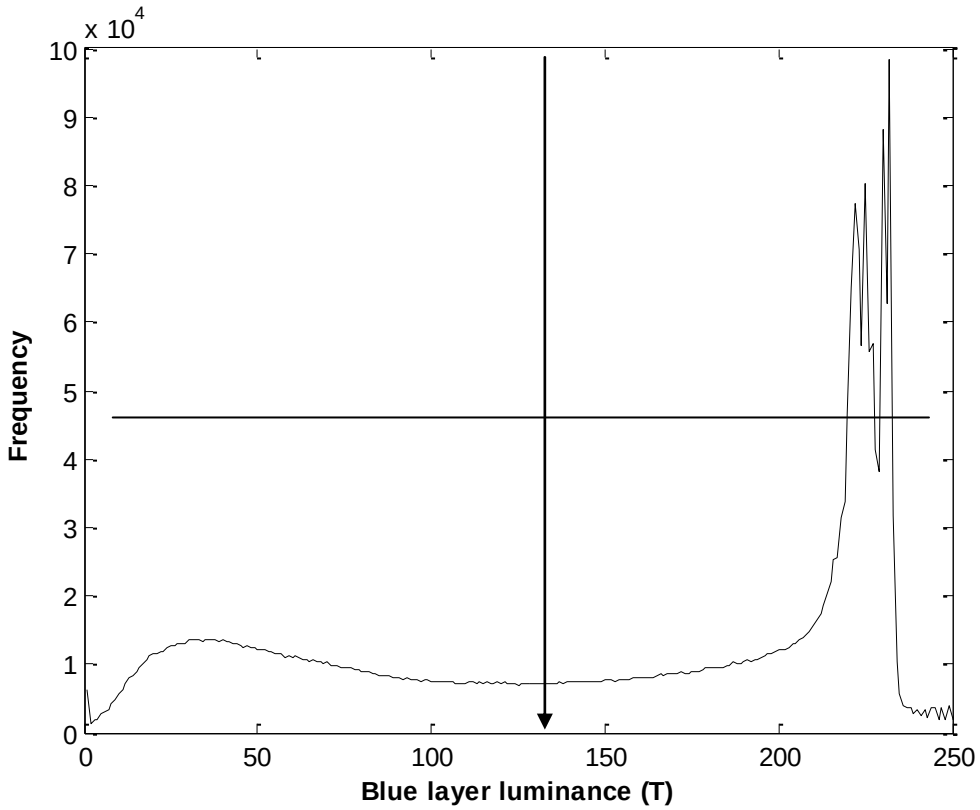

Figure 3. Luminance distribution for a single image showed as a blue component histogram generated by the script developed in MATLAB®. Sky and canopy luminance peaks can be seen at the left and right sides of the graph, respectively. A suitable threshold for clouds exclusion can be achieved in the middle, around lowest value. Cross cursor is a selector generated by the script for easy threshold selection.

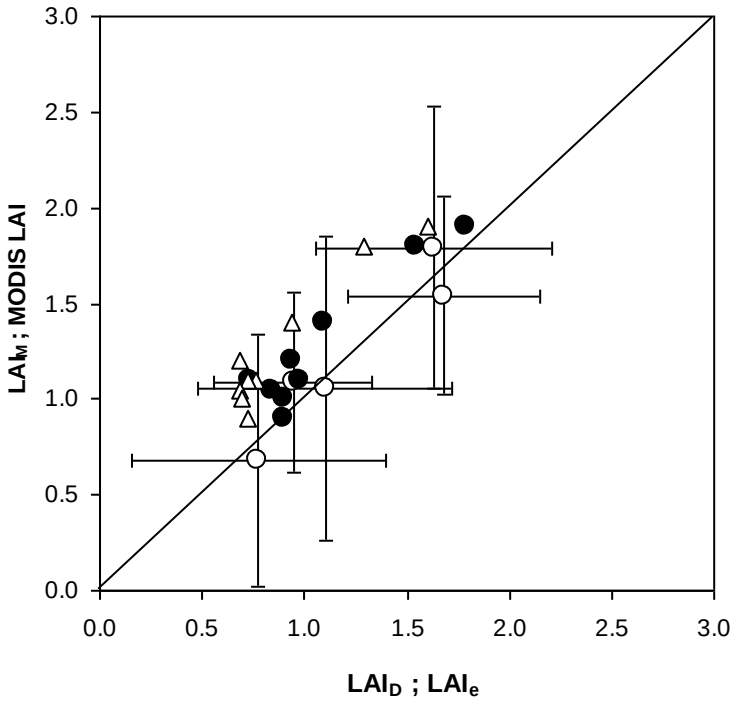

Figure 4. Comparison between LAI_M and LAI_D (open circles) for five sites in NSW; MODIS LAI and LAI_D (filed circles) and MODIS LAI and LAI_e (open triangles) for eight woodland sites in NWS and WA. Standard error bars for LAI_D *versus* LAI_M data and the 1:1 line are shown in the graph.

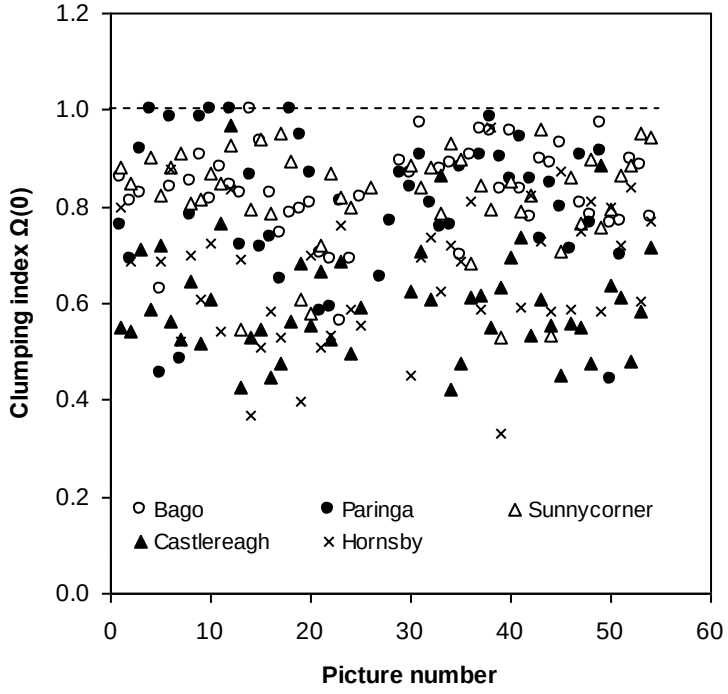

Figure 5. Calculated clumping index (Ω(0)) using formulas 2, 3 and 5 for individual images taken at five sites in NSW (n = 268).

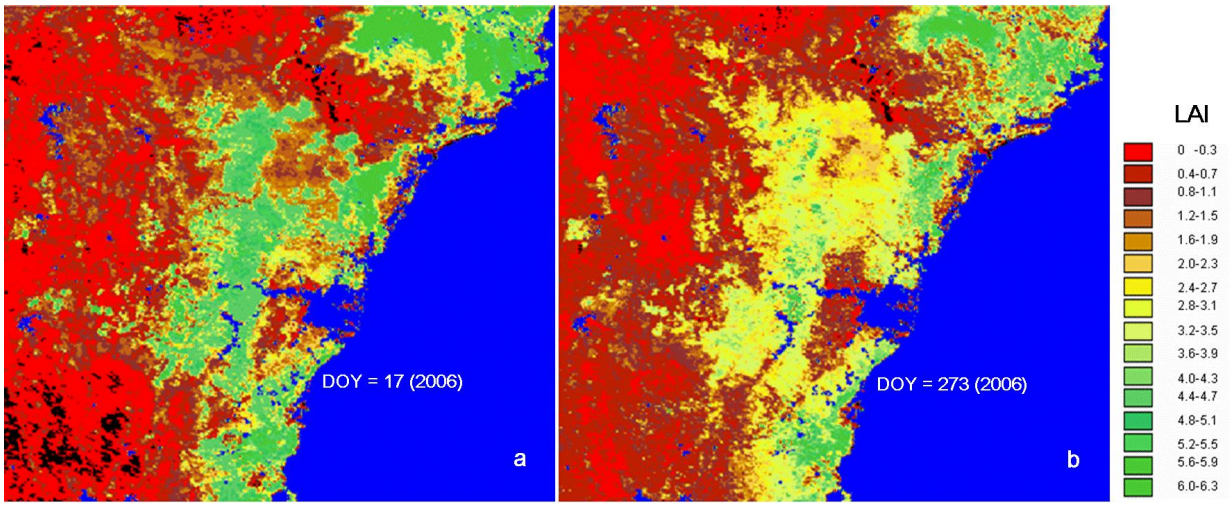

Figure 6 MODIS LAI data combined with GIS (IDRISI®) for summer (a) and spring (b) in NSW, Australia 2006.

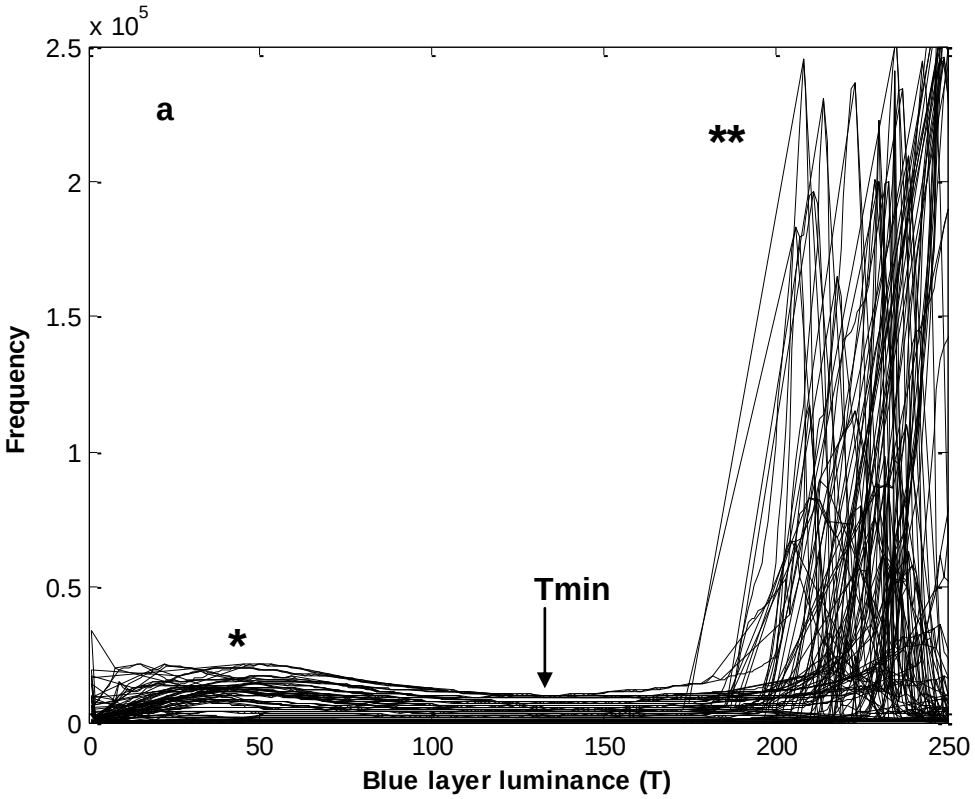

1

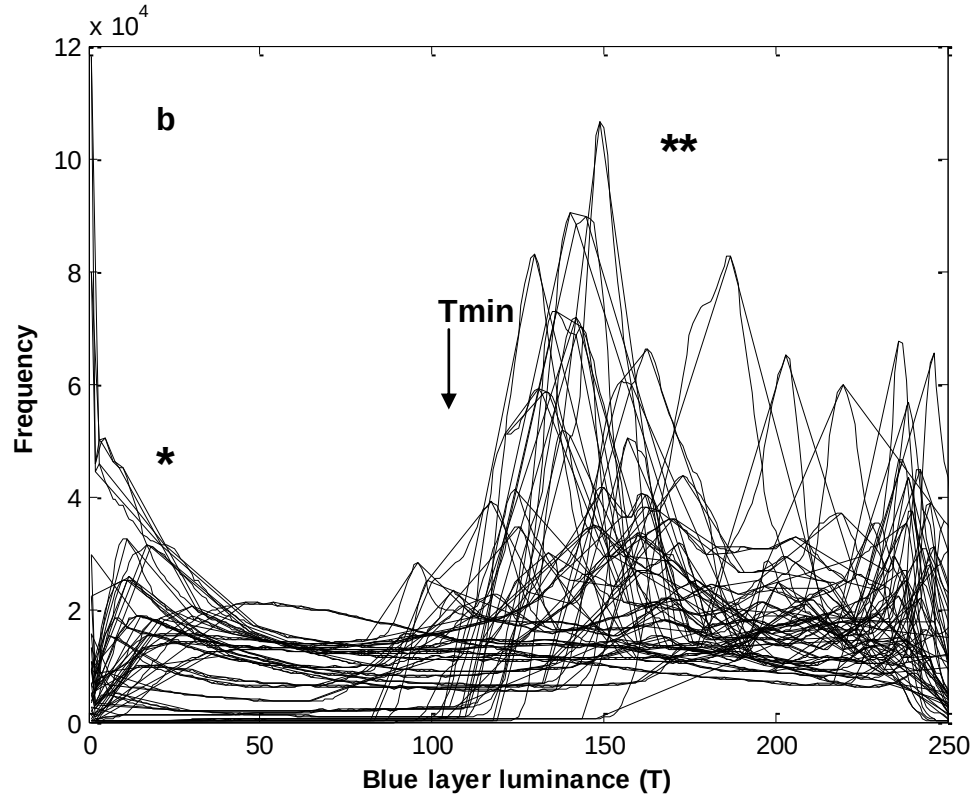

2

3 Figure 7 Histograms of blue layer luminance distributions for 50 images obtained on
4 clear days (a) and 30 images on patchy cloudy days (b) to perform a sensitivity
5 analysis of LAI_M to T. A baseline luminance threshold (Tmin) is selected at minimum
6 frequency between the peaks corresponding to sky (a) and foliage (b)
7

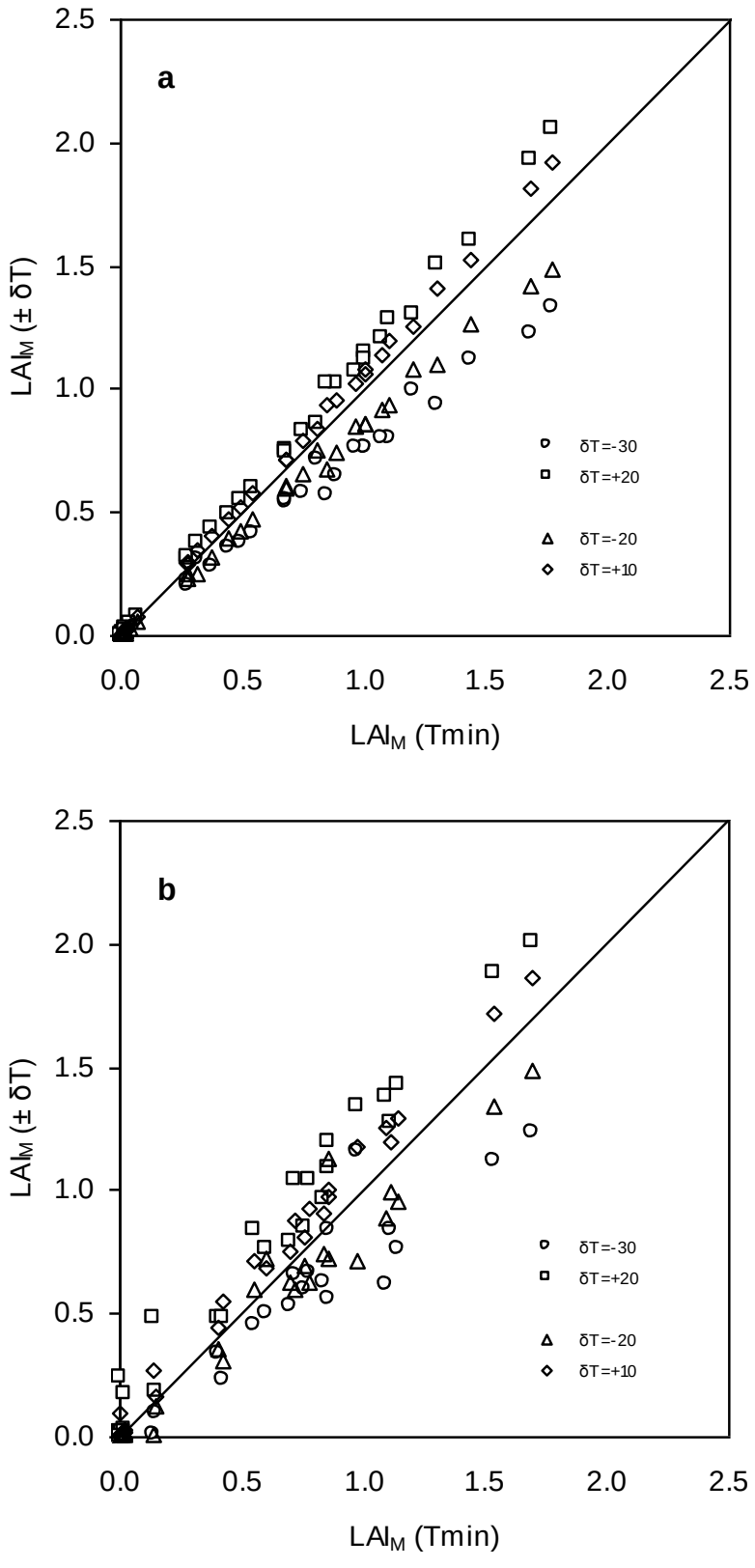

Figure 8 Sensitivity analysis of LAI_M to T conducted for 50 images on clear days (a) and 30 images on patchy cloudy days (b). The magnitude of error used were δT = -30; +20; -20 and +10. The baseline used was Tmin.

Table 2 Results of sensitivity test on LAI_M to T. The analysis is done comparing a common Tmin selected as baseline for all images obtained in clear days (T = 130; LAI_M = 0.49) and for patchy cloudy day images (T = 100; LAI_M = 0.59). Tmin corresponded to luminosity value with minimal frequency for the majority of images (Figure 7).

Clear days (n = 50); LAI_D = 0.49						
Parameters		r^2	b	RMSE	SEE	LAI_M
Tmin (baseline) vs T ±δ	δT = -30	1.00	0.75	0.03	0.037	0.38
	δT = +20	1.00	1.14	0.02	0.019	0.56
	δT = -20	1.00	0.86	0.02	0.013	0.42
	δT = +10	1.00	1.07	0.01	0.004	0.53
Cloudy days (n = 30); LAI_D = 0.68						
Parameters		r^2	b	RMSE	SEE	LAI_M
Tmin (baseline) vs T ±δ	δT = -30	0.92	0.76	0.11	0.313	0.46
	δT = +20	0.97	1.17	0.01	0.236	0.27
	δT = -20	0.95	0.89	0.10	0.244	0.52
	δT = +10	1.00	1.03	0.04	0.047	0.68